

RESEARCH

Open Access



RXLR effector genes mediate regional adaptation of *Phytophthora infestans*

Jie Zheng¹, Peng Tian¹, Wanyue Li¹, Yimeng Cao¹, Yuling Meng¹, Jiasui Zhan² and Weixing Shan^{1*} 

Abstract

Local adaptation has been a central theme of eco-evolutionary research for decades. It is generally assumed that plant pathogens are locally adapted due to their standing interactions with biotic and abiotic factors in the ecosystem. Effectors, secreted small proteins encoded by pathogens, play critical roles in host–pathogen interactions, by activating host genotype-specific resistance, suppressing plant immunity, and playing other functions. In this study, we investigated the potential involvement of RXLR effector genes in ecological adaptation by examining the simple sequence repeat (SSR), virulence, and effector profiles in *Phytophthora infestans* isolates collected from two geographic regions differing in ecological environments. Genotypic analyses with SSR markers and virulence assays showed that the pathogen from the two regions shared genetic background but differed in virulence spectrums. High-throughput sequencing and expression analysis of 24 selected *P. infestans* isolates further showed variations in the RXLR effector repertoire, ranging from 536 to 548 for each isolate and the expression of effector genes was highly associated with the accumulation of homologous sRNA. Regional specific alleles were detected at 94 RXLR effector genes, and a specific accumulation of homologous 25–26 nt sRNAs was found at 67 RXLR effector genes. Two of the regional specific RXLR effector genes were confirmed to be virulence factors. Taken together, these results suggest that genomic and epigenetic variations in RXLR effector genes contribute significantly to the ecological adaptation of *P. infestans* populations and that regional specific effector genes will help to understand the adaptive landscape of pathogens and efficient use of host resistance genes.

Keywords *Phytophthora infestans*, RXLR effector, Expression variation, Ecological adaptation, 25–26 nt sRNA, Disease resistance

Background

Pathogens have widespread impacts on ecosystem structure including the community composition, biodiversity, and species distribution, and through such impacts regulate ecosystem processes including primary production, secondary production, biogeochemical cycles,

and disturbance mechanisms (Fischhoff et al. 2020). The contribution of pathogens to ecosystems and their processes begins with their interactions with hosts, altering plant abundance, distribution, and behaviours, as well as community composition (Fischhoff et al. 2020; Mainwaring et al. 2023), which leads to rapid and reciprocal shifts in genetic structure and diversity of both host plants and pathogens and drives their co-evolution (Khavkin 2021).

Over this long-term antagonistic interaction, plant hosts continuously develop a resistance repertoire to defend against pathogens, while pathogens constantly sharpen their invasion capabilities to overcome the defense mechanisms of plants (Ngou et al. 2022). Effector, a group of small proteins secreted by pathogens, play critical roles in host–pathogen co-evolution, involved in

*Correspondence:

Weixing Shan
wxshan@nwafu.edu.cn

¹ State Key Laboratory for Crop Stress Resistance and High-Efficiency Production and College of Agronomy, Northwest A&F University, Yangling 712100, China

² Department of Forest Mycology and Plant Pathology, Swedish University of Agricultural Sciences, 75007 Uppsala, Sweden



© The Author(s) 2024. **Open Access** This article is licensed under a Creative Commons Attribution 4.0 International License, which permits use, sharing, adaptation, distribution and reproduction in any medium or format, as long as you give appropriate credit to the original author(s) and the source, provide a link to the Creative Commons licence, and indicate if changes were made. The images or other third party material in this article are included in the article's Creative Commons licence, unless indicated otherwise in a credit line to the material. If material is not included in the article's Creative Commons licence and your intended use is not permitted by statutory regulation or exceeds the permitted use, you will need to obtain permission directly from the copyright holder. To view a copy of this licence, visit <http://creativecommons.org/licenses/by/4.0/>.

overcoming host defense system, nutrient absorption, and ultimately the development of disease symptoms (Uhse and Djamei 2018; Chen et al. 2019). In addition to its role in host–pathogen interaction, effectors also contribute to other biological and ecological functions, such as regulating osmotic pressure (Kasmi et al. 2018), antimicrobial activities (Snelders et al. 2020), and microbiota composition (Cai et al. 2023).

In addition to sequence characteristics, the contribution of effectors to host–pathogen interactions also depends on their expression and successful delivery to host cells. Many effector genes are not constitutively expressed. Their expression and delivery are induced upon contact with the host and involve many biotic and abiotic environments. Abiotically, it has been documented that the expression and delivery of effectors are influenced by climatic conditions, such as air temperature, light spectrum, and humidity (Goel et al. 2008). For example, increased translocation of effectors into host plants was detected during *Pseudomonas syringae* pv. *tomato* DC3000 infection in *Arabidopsis* at elevated temperature (Huot et al. 2017), and enhanced UV-B radiation can down-regulate the expression of disease-causing genes in *Magnaporthe grisea* (Huang et al. 2019). In *P. infestans*, both UV radiation and temperature can regulate the expression and evolution of *Pi02860* (Yang et al. 2022). The ability of effector proteins AvrE and HopM1 to cause water soaking requires high atmospheric humidity in *P. syringae* (Xin et al. 2016). Climatic conditions can also alter mutation and selection of effector genes, leading to spatial heterogeneity across different ecosystem (Velásquez et al. 2018). For example, population genetic analyses showed that *P. infestans* effector genes, such as *Avr1* (Shen et al. 2021), *Avr2* (Yang et al. 2020), *Avr3a* (Yang et al. 2018), and *Avr4* (Waheed et al. 2021), were strongly associated with annual mean temperature. Under UV radiation, the mutation rate increased significantly in *Escherichia coli* at the genomic scale (Shibai et al. 2017).

From a biological perspective, effector gene expression can be regulated by internal interactions with other genes in the genome (i.e., epistasis; Phan et al. 2016) or external interactions with metabolites secreted by other species (Bever et al. 2012). For example, as a common regulator of gene expression in eukaryotes (Castel and Martienssen 2013), small RNAs (sRNAs), especially 25–26 nt sRNAs, are associated with silencing of homologous RXLR effector genes in *Phytophthora* pathogens (Jia et al. 2017; Zhang et al. 2019) and the components in this gene silencing pathway are shared among species (Vetukuri et al. 2011). Co-immunoprecipitation (Co-IP) assays showed that the classes of 20–22 nt and 24–26 nt sRNAs could bind to PiAGO1 and PiAGO4 and modify their

translation, respectively, confirming the regulatory function of sRNAs (Åsman et al. 2016). In oomycete, abundant endogenous sRNAs, such as 21 nt and 25 nt sRNAs, were detected in *P. infestans*, *P. sojae*, *P. parasitica*, and *P. ramorum* (Vetukuri et al. 2012; Qutob et al. 2013; Jia et al. 2017) and silencing of *Avr3a* (Qutob et al. 2013) and *Avr1b* (Wang et al. 2019) in *P. sojae* was confirmed to be associated with homologous sRNA accumulation. Further sequence analysis showed that some flanking regions of effector genes also involved in the epigenetic processes of expression regulation (Wang et al. 2020). Since RNA-seq and sRNA-seq results showed a clear negative correlation between expression of RXLR effector genes and homologous 25–26 nt sRNA accumulation (Jia et al. 2017), the expression levels of effector genes could be directly reflected by their homologous 25–26 nt sRNA accumulation.

Our research on effector genes has mainly focused on functional analysis of their pathogenicity aspects such as virulence/avirulence (Wang et al. 2023) and how they evade host recognition by sequence variation (*Avr1*, *Avr4*, *Avr3a*, *Pi20303*; Du et al. 2018; Du et al. 2021; Shen et al. 2021; Waheed et al. 2021), but knowledge about how epigenetics and abiotic factors influence evolutionary adaptation of effectors is largely unknown. Especially, we generally lack information on whether the local adaptation of pathogens to ecological niches is associated with regional specific variation in genomic signatures and/or expression of effector genes. Therefore, exploring regional variation in genomic characteristics and expression of effector genes and the contribution of abiotic environments to the variation can provide clues for understanding the role of pathogen effectors in ecological function and resilience. This knowledge is also important in the efficient deployment of resistance genes for sustainable crop production.

In this study, we combined population genomics and potato (*Solanum tuberosum*)-*P. infestans* interactions to address these questions. Potato is one of the most important non-grain food crops and plays a crucial role in the world food security system (Guo et al. 2023). However, primary production of potato can be severely threatened by *P. infestans*, the notorious pathogen that caused the Irish famine in 1840s (Lal et al. 2019). Under the favored temperature and humidity conditions, *P. infestans* can multiply rapidly and destroy an entire potato crop in a field within days. The pathogen encodes a large number of secreted effector proteins, including the most important RXLR effectors that contain a conserved RXLR (Arg-any amino acid-Leu-Arg) domain (Rehmany et al. 2005). It is estimated that the ~240-Mb genome consists of 563 annotated RXLR effector genes, and most of them are located in the

rapidly evolving, repeat-rich but gene sparse regions (GSR; Haas et al. 2009), providing unique niches for quick mutation and evolution.

It's common that the field performance of potato varieties for late blight resistance differs among regions, suggesting regional adaptation of *P. infestans* populations and the potential role RXLR effector genes may play. To investigate potential involvement of RXLR effector genes in mediating regional adaptation of *P. infestans* populations, we collected 155 *P. infestans* isolates from Tianshui, Gansu (TSGS) and Weining, Guizhou (WNGZ), and performed high-throughput sequencing on 24 of these isolates (21 of which were dominant genotypes in both regions). TSGS and WNGZ are among the main potato producing areas in China and differ substantially in ecological environments. TSGS in Northwest China has moderate temperatures and little rainfall, while WNGZ in Southwest China has lower-temperature and more rainfall during the potato planting season. The prevalence of late blight differs significantly between the two regions.

The specific objectives of the study were to (1) investigate the population genetic structure of *P. infestans* populations in SSR markers and RXLR effector repertoire; (2) identify regional specific RXLR effector genes at genomic and transcriptional levels; and (3) determine ecological and genetic environments contributing the regional differentiation of effector genes.

Results

Shared *P. infestans* genotypes with variation in virulence in distant regions

A total of 8 genotypes were identified from 155 *P. infestans* isolates which were collected from potato varieties Longshu 10, Nongtian 1, Tianshu 10, Tianshu 11, Tianshu 12, Tianshu 13, Weiyu 5, Weiyu 3, and Qingshu 9 cultivated in TSGS and WNGZ (Additional file 1: Table S1). The genotypes Gt1 and Gt2 dominated in both regions (Additional file 2: Figure S1a, b). Two (Gt6 and Gt7) genotypes appeared to be regional specific, one in each region. All other six genotypes were detected in both regions, suggesting long-distance transmission of *P. infestans*.

Virulence assays of 24 *P. infestans* isolates (12 from each region) on potato cultivar Qingshu 9 showed that 16 of the isolates successfully infected potato leaves (Additional file 1: Table S2, S3). However, symptoms caused by the WNGZ isolates appeared to be more aggressive than those caused by the TSGS isolates, resulting significantly larger lesions (Fig. 1a, b).

Significant variations in *P. infestans* RXLR effector repertoire

Due to the unsuccessful library construction for 5 *P. infestans* isolates (PL1007, PL1011, PL1029, PL1038, and PL6080), we performed whole genome re-sequencing for 19 of them, including 8 from TSGS and 11 from WNGZ (Additional file 1: Table S4). RXLR effector repertoire in the isolates ranged from 536 to 548 (Fig. 2a). Among them, 521 annotated RXLR effector genes were

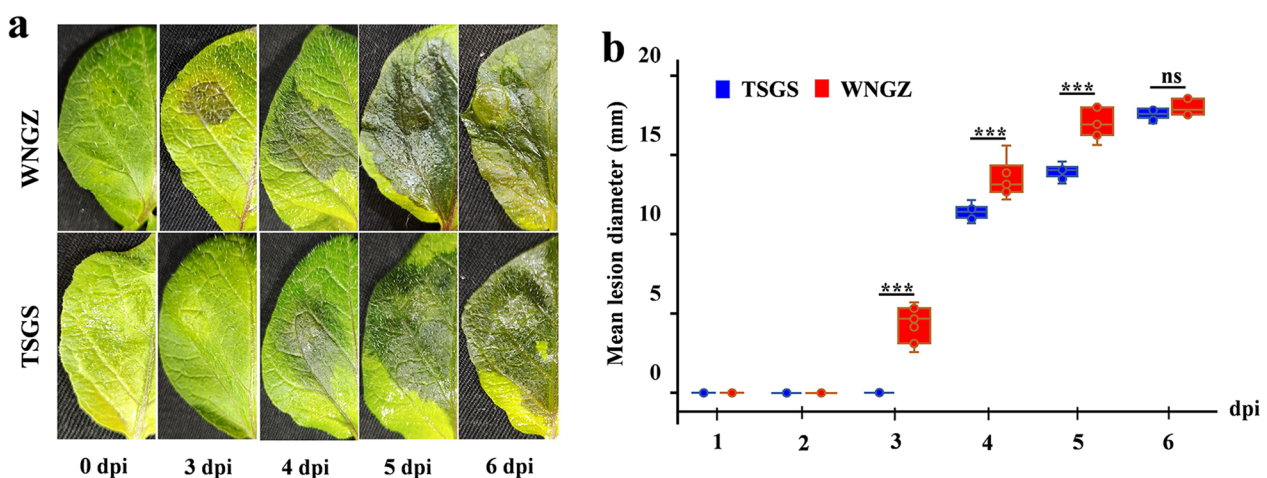


Fig. 1 Late blight phenotypes and differential lesion development by *P. infestans* isolates from TSGS and WNGZ. **a** Disease phenotype upon infection. A total of 16 isolates (9 from TSGS and 7 from WNGZ) were examined, with lesion diameters induced by the WNGZ isolates significantly larger. The figure shows the disease phenotype of isolate PL1024. **b** Development of lesion diameters. The lesions were presented as the mean \pm SE of at least 3 independent biological replicates. Statistical significance was assessed by Student's *t*-test. ns, not significant. *** $P < 0.001$

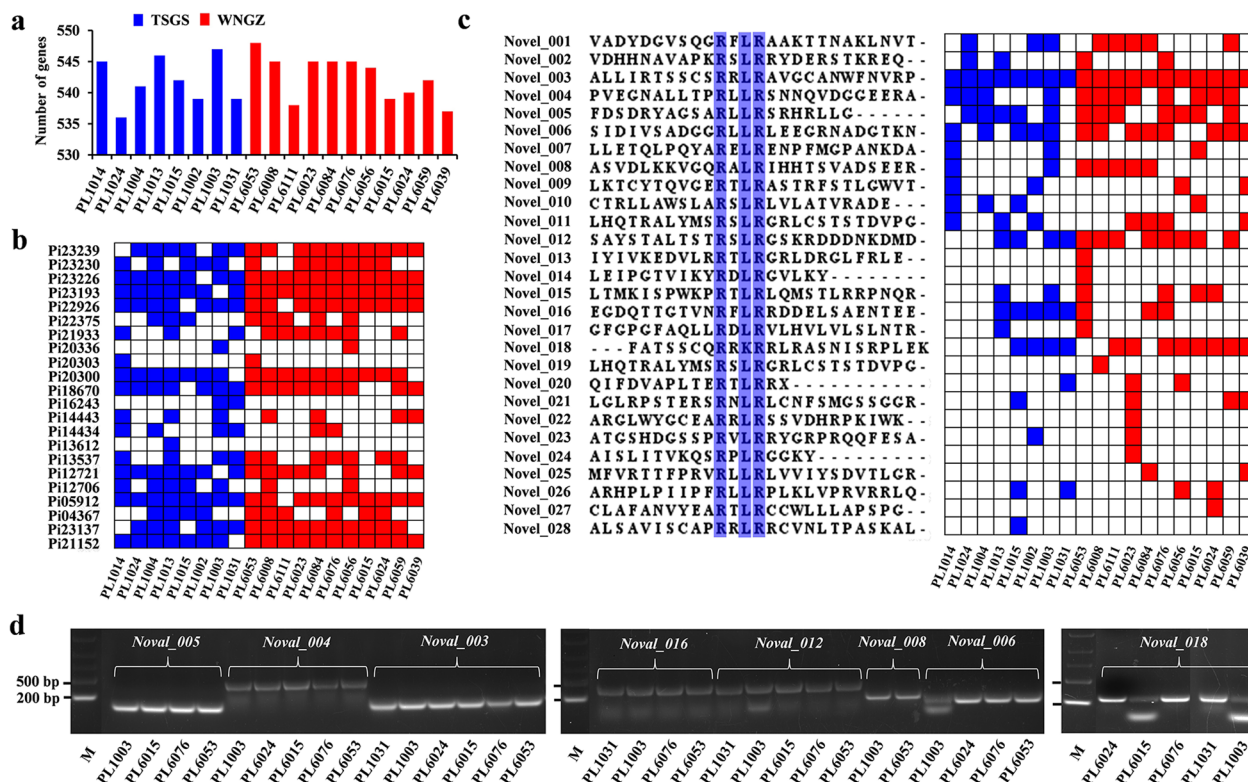


Fig. 2 RXLR effector repertoire in 19 sequenced *P. infestans* isolates. **a** Number of RXLR effector genes in each isolate, including annotated genes and predicted novel genes. **b** PAV of 22 annotated RXLR effector genes. The colored grids represent the existence of the effector genes in the corresponding isolate. Blue and red represent the isolates from TSGS and WNGZ, respectively. **c** Conserved amino acid sequences (left) and distribution (right) of novel RXLR effector genes. **d** Validation of the novel RXLR effector genes. Novel RXLR effector genes were verified by PCR amplification with genomic DNA

mapped to all 19 isolates, while 20 functionally characterized effector genes, including *Avr1* and *Avr3b*, were completely missing from the genomes. Among the 19 genomes, 22 RXLR effector genes showed present or absent variations (PAV; Fig. 2b). However, there is no regional specific PAV in RXLR effector genes between the genomes from two regions.

We also examined novel RXLR effector genes not annotated in each genome by performing de novo assembly of the unmapped Illumina reads. From the 42.7 Mb contigs that did not map to the reference genome, 28 novel RXLR effector genes were identified (Fig. 2c). Except for *Novel_003*, most of the novel effector genes also showed PAVs among the sequenced isolates. Eight of the novel effector genes which present in most isolates were confirmed by PCR (Fig. 2d; Additional file 1: Table S5).

RXLR effector genes exhibiting regional differences

Based on the mapping results, a total of 584,869 SNPs were identified among the 19 genomes. Of which 46,405 (7.9%) were enriched in RXLR effector genes (gene body and 1 kb flanking regulatory sequences). Phylogenetic

and principal component analysis (PCA) of the SNPs in the whole genomes (Additional file 2: Figure S2a) showed that the TSGS and WNGZ isolates could not be separated according to their geographic origin (Additional file 2: Figure S2b–d), further suggesting close genetic relationship between *P. infestans* from the two areas. However, phylogenetic analysis of SNPs from RXLR effector genes showed that *P. infestans* isolates tended to be clustered according to their geographic origins, with some exceptions such as PL1015 (TSGS isolate) and PL6111 (WNGZ isolate; Additional file 2: Figure S2e).

To identify variant sites that represent the differences among 19 *P. infestans* isolates, the consistent SNPs/Indels among all isolates were filtered out. 644 non-synonymous SNPs and 84 InDels (at least one individual was different with the other 18) were identified in the coding regions of 244 and 63 RXLR effector genes, respectively (Fig. 3a; Additional file 2: Figure S3a). Among them, no variant sites that were present in all isolates of one region but absent in all isolates of another region were detected. After calculating the number of SNPs/Indels in the isolates (Additional file 1: Table S6), we considered a variant

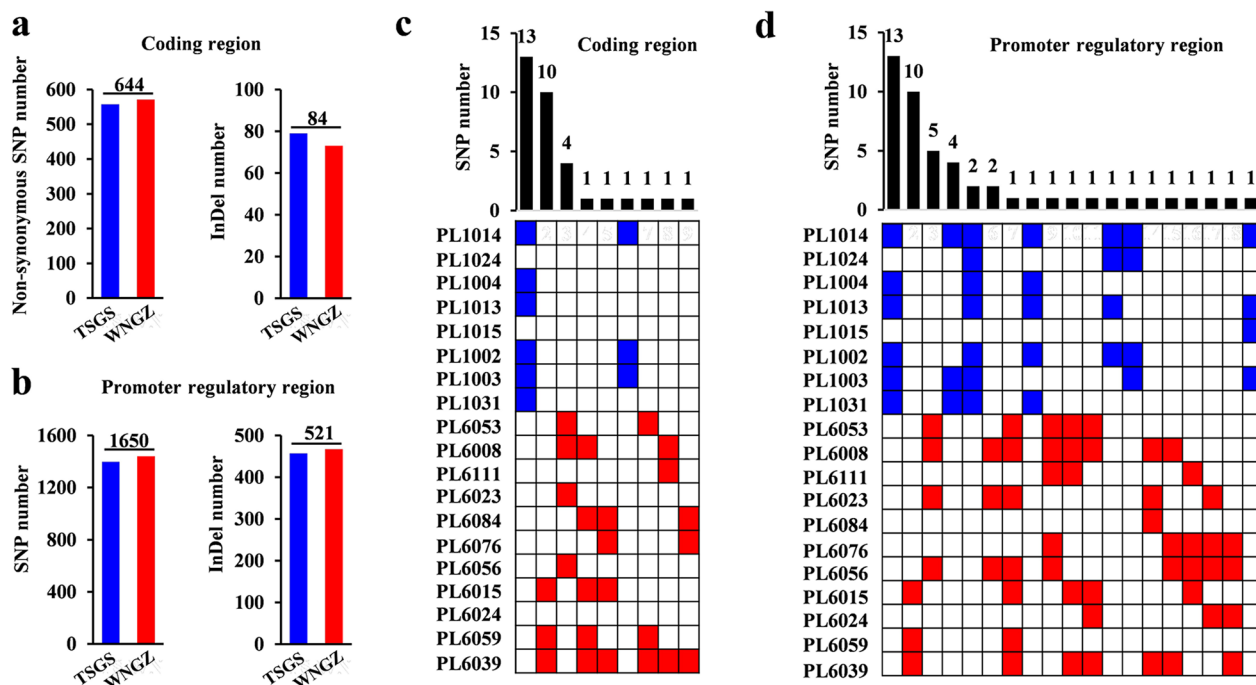


Fig. 3 Sequence variations in *P. infestans* RXLR effector genes. **a, b** Number of SNPs (left) and InDels (right) in coding regions and promoter regions of effector genes in TSGS and WNGZ isolates. The number above the black line represents the total SNPs and InDels, which is the union of SNPs and InDels in each isolate. **c, d** Number and distribution of regional specific SNPs in coding regions and promoter regions. Only part of the whole picture was taken for display. The histogram shows the number of SNPs, and the colored grids represent the existence of SNPs in the corresponding isolates

that appeared at least three isolates in one region but not in another region to be regional specific. Accordingly, 33 SNPs and 4 InDels showed regional specific (Fig. 3c; Additional file 2: Figure S3c). For instance, the known effector gene *Avr-Smira2* exhibited consensus SNPs in six of nine genomes in the TSGS isolates, resulting in a Gly to Arg amino acid change at position 55 (Additional file 2: Figure S3e).

Analyses of sequence variation in the promoter regions of the RXLR effector genes showed 1650 (0.28%) SNPs and 521 (0.68%) InDels in the regulatory sequences of 385 and 251 RXLR effector genes (Fig. 3b), respectively. The number of differential SNPs and InDels in each genome ranged from 648–860 to 247–310, respectively (Additional file 2: Figure S3b). Among them, we identified 32 and 40 regional specific mutations between the TSGS and WNGZ isolates, respectively (Fig. 3d; Additional file 2: Figure S3d), including the known effector genes *Avr-Smira1*, *Avr-amr1*, and *Pi22798* (Additional file 2: Figure S3f). Further analyses confirmed that the transcript levels of WNGZ-specific *Pi12721*, *Pi23048*, *Pi15109*, and TSGS-specific *Pi19302* exhibited significant regional signatures during plant infection. *Pi12721* and *Pi15109* were highly expressed

in the WNGZ isolates at 12 hpi and 48 hpi, respectively (Additional file 2: Figure S4a, c). *Pi19302* was continuously expressed in the WNGZ isolates during infection, and its expression level was significantly higher than that in the TSGS isolates (Additional file 2: Figure S4d). *Pi23048* displayed low expression only in the mycelia of the TSGS isolates (Additional file 2: Figure S4b). These results suggest that the contribution of regulatory sequences to the expression variation of regional specific effectors is likely limited.

The Indel mutations identified in RXLR effector genes ranged from 1 to 51 bp in length, with the majority (86.15%) shorter than 15 bp. The 1-bp and 10-bp InDels were more frequent in the flanking regulatory sequences of RXLR effector genes (Additional file 2: Figure S5a). Further analysis showed that the 10-bp InDels were widely distributed (14%) in the regulatory sequences of all genes in *P. infestans* genome (Additional file 2: Figure S5b), and their frequency was similar to that in the RXLR effector genes (12%). However, there was no regional specific 10-bp InDels in the promoter regions of these effector genes.

Expression variation in RXLR effector genes

We analyzed the accumulation of 25–26 nt sRNAs homologous to RXLR effector genes during vegetative growth in 24 *P. infestans* isolates by sRNA-seq (Additional file 1: Table S7) and performed transcriptome sequencing of RXLR effector genes (Additional file 1: Table S8). The results showed that the expression of most RXLR effector genes (~70%, 390–425 genes) was repressed during the vegetative growth stage (Fragments

per Kilobase Million, FPKM < 1) (Additional file 2: Figure S6a). Among the 563 annotated RXLR effector genes, 223 (39.6%)–369 (65.5%) were detected with homologous 25–26 nt sRNAs (RPKM > 1) in each *P. infestans* isolate (Fig. 4a; Additional file 2: Figure S6b). Among them, the expression of 197–298 (79.8–88.3%) RXLR effector genes was completely silenced (Fig. 4a).

To identify differential expression of RXLR effector genes between the two regions, we examined variations

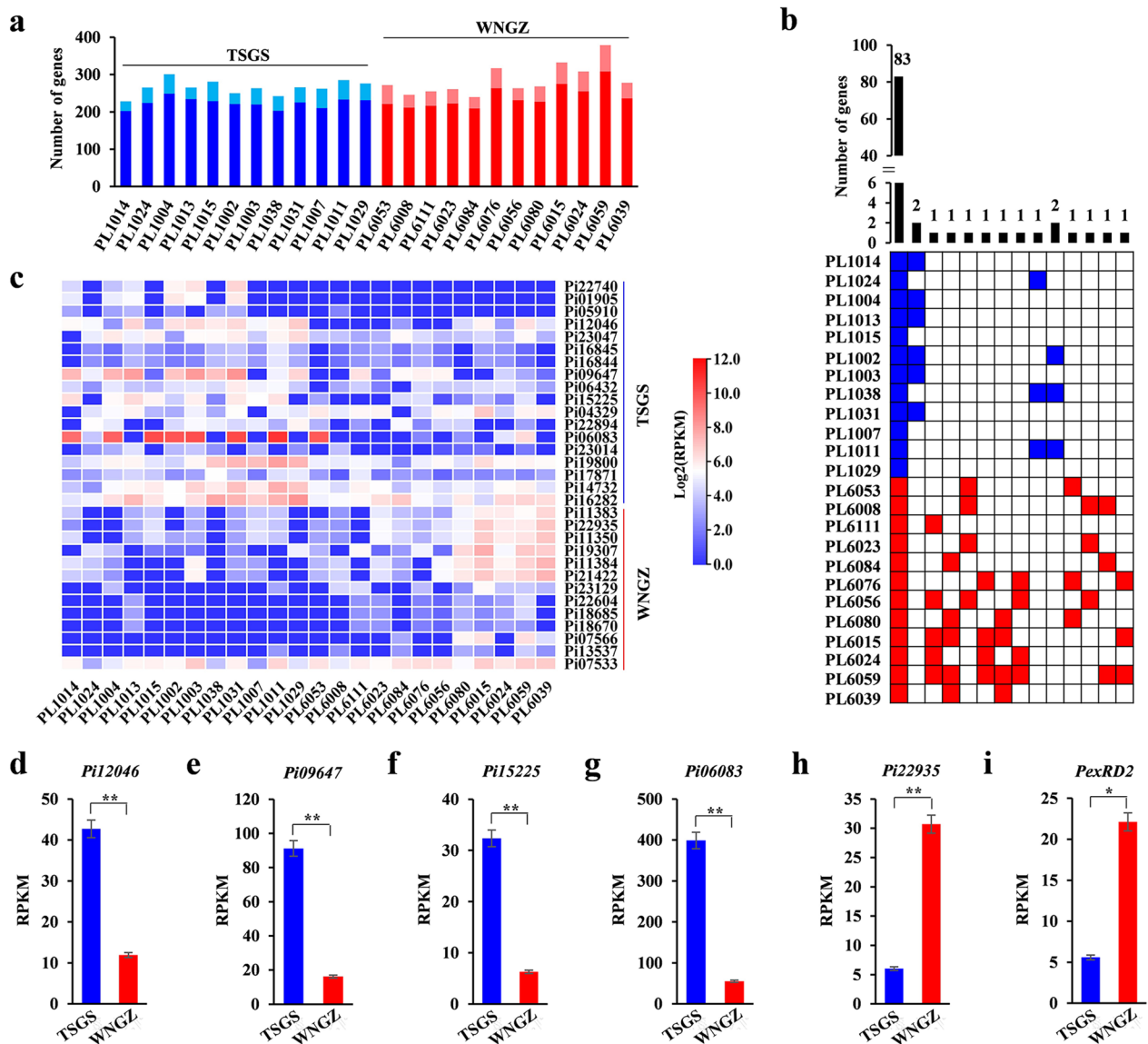


Fig. 4 Regional specific RXLR effector genes enriched with homologous 25–26 nt sRNA. **a** Number of effector genes enriched with sRNAs. Blue/light blue and red/light red represent the number of silent/expressed effector genes from TSGS and WNGZ isolates, respectively. **b** Number and distribution of regional specific effector genes. The figure above the bar graph represents the number of genes, and the colored and white grids below represent the present or absent accumulation of sRNAs at these genes in the isolate. **c** Heatmap visualization of sRNA accumulation levels of regional specific effector genes. **d–i** Differential accumulation of 25–26 nt sRNAs homologous to effector genes *Pi12046*, *Pi09647*, *Pi15225*, *Pi06083*, *Pi22935*, and *PexRD2* in TSGS and WNGZ isolates. Statistical significance was assessed by Student's *t*-test. **P* < 0.05, ***P* < 0.01

in sRNA accumulation that are detected in at least three isolates from the same region. We identified 277 and 295 sRNA-accumulating RXLR effector genes in TSGS and WNGZ isolates, respectively, with 260 being shared in both regions (Additional file 2: Figure S6c). There were 83 RXLR effector genes that accumulated with the 25–26 nt sRNAs across all isolates (Fig. 4b). Based on their accumulation with homologous 25–26 nt sRNAs in vegetative hyphae, it was notably found that 5 and 10 RXLR effector genes were inferred to be specifically expressed in TSGS and WNGZ isolates, respectively (Fig. 4b). For instance, the most regional specific genes including the TSGS-specific *Pi22740* and *Pi01905*, and the WNGZ-specific *Pi07566* showed abundant accumulation of the 25–26 nt sRNAs in isolates from one region but rare from another region. In addition to the qualitative difference in presence or absence, we also found quantitative differences in sRNA accumulation levels between the two regions. In the TSGS isolates, 18 RXLR effector genes accumulated more homologous 25–26 nt sRNAs, whereas 13 accumulated more homologous 25–26 nt sRNAs in the WNGZ isolates (Fig. 4c). For example, *Pi12046*, *Pi09647*, *Pi15225*, and *Pi06083* accumulated more 25–26 nt sRNAs in the TSGS isolates, but *Pi22935* accumulated more 25–26 nt sRNAs in the WNGZ isolates (Fig. 4d–h). *PexRD2* family is a class of RXLR effector genes (Haas et al. 2009), in which five members significantly accumulated more sRNAs in the WNGZ isolates than that in the TSGS isolates (Fig. 4i). Further expression analysis suggested that the high-level accumulation of homologous 25–26 nt sRNAs at *Pi09647* and *Pi12046* in the TSGS isolates, as well as *Pi22935* and *Pi18670* in the WNGZ isolates, were negatively associated with the expression of the corresponding RXLR effector genes throughout or at specific stages of infection (Additional file 2: Figure S7a–d).

Enriched accumulation of homologous 25–26 nt sRNA at flanking regulatory sequences of RXLR effector genes

Except for the coding regions, we also found obvious accumulation of 25–26 nt sRNAs at the flanking regions of RXLR effector genes. Overall, there was no significant difference in the number of RXLR effector genes that accumulate homologous 25–26 nt sRNAs in the coding regions, upstream and downstream regulatory sequences (Fig. 5a). However, the abundance of homologous 25–26 nt sRNAs in the upstream and downstream regions was significantly higher than that at coding regions in each isolate (Fig. 5b; Additional file 2: Figure S8a), indicating a higher degree of 25–26 nt sRNA accumulation at the flanking regions of RXLR effector genes.

We further examined the accumulation of 25–26 nt sRNA homologous to the upstream regulatory sequences of RXLR effector genes and compared it with the gene expression level in each isolate at the vegetative growth stage. The results showed that 227–345 RXLR effector genes accumulated homologous 25–26 nt sRNAs in the promoter region and 74.7–83.0% of them were silenced (Fig. 5c). We also found that four and five regional specific RXLR effector genes differentially accumulated homologous 25–26 nt sRNAs in TSGS and WNGZ isolates, respectively (Fig. 5d). It's also notable that 24 and 3 RXLR effector genes accumulated more homologous 25–26 nt sRNAs than others in TSGS and WNGZ isolates (Fig. 5e), respectively. The TSGS-specific RXLR effector genes *Pi15225*, *Pi12046*, *Pi06083*, *Pi04329*, *Pi01905*, and *Pi09647* accumulated more homologous 25–26 nt sRNAs in both promoter and coding regions (Fig. 5f–k). Further exploration revealed that there was no correlation between sequence variations in the promoter region and the accumulation of sRNA.

RXLR effector genes differentially accumulated with homologous 25–26 nt sRNAs were virulence factors

To examine whether the sRNA-associated RXLR effector genes contribute to the virulence of *P. infestans*, the regional specific RXLR effector genes *Pi22740* and *Pi04329*, and region-shared effector genes *Pi18487*, *Pi08399*, *Pi04350*, and *Pi17214*, all with significant accumulation of homologous 25–26 nt sRNAs, were cloned and transiently expressed in *Nicotiana benthamiana* by agroinfiltration assays. After 5 days post-inoculation with *P. infestans* zoospores, *N. benthamiana* leaves transiently overexpressed with RXLR effector genes all developed significantly larger lesions than the *GFP* control (Fig. 6a, b). The results showed that the two regional specific RXLR effector genes differentially accumulated homologous 25–26 nt sRNAs were virulence factors, suggesting their contribution to regional specific pathogenicity of *P. infestans*.

Discussion

Identical genotypes were captured in isolates sampled from two areas approximately 1200 km apart, consistent with the high and long gene flow reported in the pathogen (Cooke et al. 2012). Gene flow homogenizes a species' genetic variation that would otherwise accumulate due to geographic isolation (MacDonald et al. 2020). In *P. infestans*, gene flow can occur naturally through the movement of propagules or anthropogenically through the exchange of plant materials (Gao et al. 2020). For example, based on detecting the same SSR genotypes as we used, Tian et al. (2016) documented that gene flow of

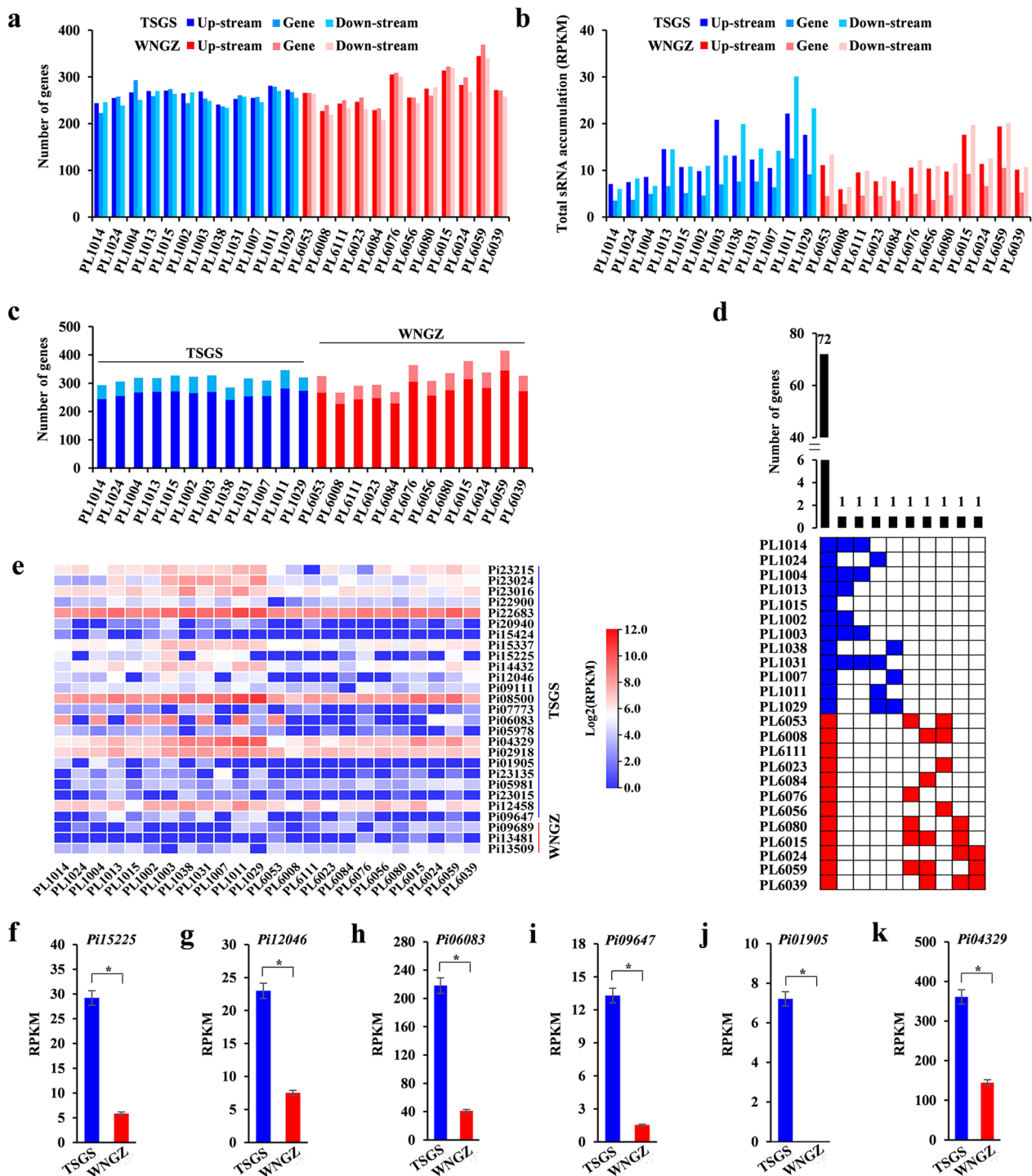


Fig. 5 Accumulation of homologous 25–26 nt sRNAs in the promoter region of RXLR effector genes. **a** Number of effector genes with sRNA accumulation in the upstream, downstream, and coding regions. **b** Average accumulation level of sRNA homologous to effector genes. **c** Number of effector genes enriched with sRNAs in the promoter regions. **d** Number and distribution of regional specific effector genes. **e** Heatmap visualization of sRNA accumulation levels of regional specific effector genes. **f–k** Differential accumulation of homologous 25–26 nt sRNAs in effector genes *Pi15225*, *Pi12046*, *Pi06083*, *Pi09647*, *Pi10905*, and *Pi04329* in TSGS and WNGZ isolates. Statistical significance was assessed by Student’s *t*-test. ns, not significant. **P* < 0.05

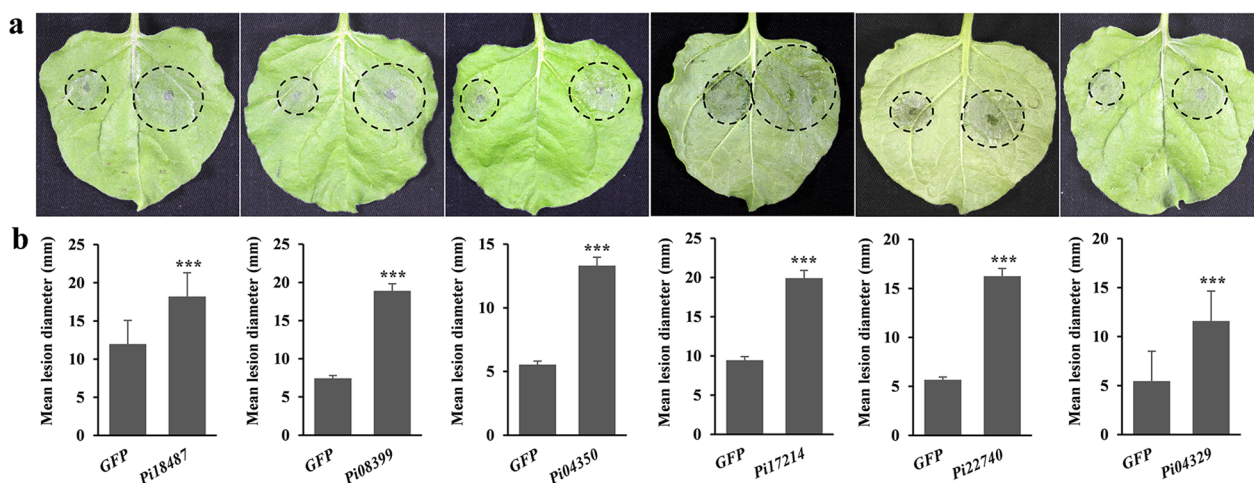


Fig. 6 Transient overexpression of RXLR effector genes enhanced plant susceptibility to *P. infestans* infection. **a** Phenotypes of *N. benthamiana* leaves infected with *P. infestans*. GFP was transiently expressed on the left of the detached leaves, and the effector was transiently expressed on the right. Photos were taken at ~7 days post inoculated with *P. infestans* zoospores. **b** Average lesion area of leaves expressing GFP and the effectors. The lesions were presented as the mean \pm SE of at least 20 independent biological replicates. Statistical significance was assessed by Student's *t*-test. *** $P < 0.001$

the pathogen can also occur among distant *P. infestans* populations.

Conflicting to the population genetic structures in SSR markers, significant spatial population differentiation was detected between the two pathogen samples in RXLR effector genomes, consistent with hypothesis of enhancing evolution in genomes involved in host–pathogen interactions and results from previous studies in *P. infestans* (Yang et al. 2020; Shen et al. 2021; Waheed et al. 2021) and other pathogens (Mandal et al. 2022). RXLR effectors of *P. infestans* are mainly located in highly variable regions of the genome surrounded by transposable elements (Haas et al. 2009), allowing the pathogen to generate large amounts of variation including continuous detection of novel effectors and rapidly adapt to the changing biological environments such as resistant genes developed in the plant host (Rietman et al. 2012). Cooke et al. (2012) performed de novo assembly and revealed six candidate RXLR effector genes that were not present in the reference genome. Using the same methods, we identified a total of 28 novel RXLR effector genes in the sequenced isolates (Fig. 2c). Interestingly, 27 novel RXLR effector genes are present in various combinations in all isolates, suggesting that recombination may also contribute to the generation of genetic variation in the effector genes of *P. infestans*. In terms of disease management in primary food production, this result highlights the importance of exploring the spatial distribution of RXLR effector genes according to ecological context and well explains the lasting efforts in this research field (Gilroy et al. 2011).

We found that 34 and 62 RXLR effector genes contain regional specific variations in the coding or promoter regulatory regions (Fig. 3c, d; Additional file 2: Figure S3c, d). Polarized population differentiation of SSR marker loci and effectormics as well as the regional specific variation in RXLR effector repertoires also provide strong evidence for local adaptation of the functional genes, contributing to the differences in the frequency and severity of late blight epidemics between WNGZ and TSGS (Todd et al. 2022). Different potato varieties were used in the two regions (Additional file 1: Table S1). These varieties may have different *R* genes, thereby contributing to the observation of regional differentiation. However, typically only a limited number of effectors are involved in resistance in a given variety (Vleeshouwers and Oliver 2014), and the contribution of this host variation to the observations, if any, is expected to be small. Furthermore, similar spatial differentiation in effector genes was also found when we only used the pathogen genome from potato variety Qingshu 9 grown in both regions.

Although host effects cannot be completely ruled out, we believe that ecological environments, especially climatic factors, also play an important role in the development of population differentiation in pathogen effector genes. Climatic conditions such as temperature, humidity, and ultraviolet radiation vary greatly between the two potato producing areas, which can generate a multifaceted impact on the function and evolutionary development of effector genes, and thus on the adaptation and epidemics of the pathogen (Cheng et al. 2019).

Genetically, climatic conditions can directly modulate the generation and preservation of genetic variation in effector genes by altering mutation rates. It can indirectly affect the generation and maintenance of genetic variation through changes in pathogen population size and reproductive strategies and efficiency. For example, temperature can affect the thermal stability of DNA molecules, thereby affecting the mutation rate of the genome including effectoromics during replication (Marguet and Forterre 1994), while ultraviolet radiation is a well-known mutagen that can induce mutations in effectors and other genes (Rastogi et al. 2010), generating spatial population differentiation of effectors along temperature gradients and altitudes in *P. infestans* (Yang et al. 2022) and many other pathogens (Matsuba et al. 2013). Epigenetically, climatic conditions can also moderate the expression of effectors directly such as by turning on/off promoters (Singh et al. 2014), or indirectly by regulating the production of translational regulators such as homologous sRNAs (Zhang et al. 2016), affecting their functional efficiency during host–pathogen interactions.

Indeed, we found strong evidence that gene expression polymorphisms contribute to the functional diversity of effector genes and potential pathogen adaptation to ecological niches and their expression is associated with accumulation of homologous sRNAs. In *P. infestans* (Vetukuri et al. 2012), as well as in *P. sojae* (Qutob et al. 2013), 25–26 nt sRNAs can silence RXLR effector, and we found that most (79.8–88.3%) of the RXLR effector genes that accumulate homologous 25–26 nt sRNAs in our study were unexpressed at mycelium stage (Fig. 4a), which enables the pathogen to produce effector proteins as needed to maximize energy efficiency (Xu et al. 2022). Furthermore, the accumulation of these homologous sRNAs in effector genes was regional specific. Although we identified 21 regional specific sRNA-associated RXLR effector genes in both the TSGS and WNGZ isolates, the total amount of sRNAs homologous to RXLR effector genes in the TSGS isolates was significantly higher than that in the WNGZ isolates (Additional file 2: Figure S8b). We believe that this differential pattern of sRNA accumulation between the pathogen isolates from the two regions may also exist during the infection stage. Due to the negative association between sRNA accumulation and pathogenicity (Qutob et al. 2013; Wang et al. 2019), this result indicates that the pathogen from TSGS causes less disease than that of WNGZ. On the other hand, it is interesting to find that the total expression levels of RXLR effector genes were not significantly different between the two regions (Additional file 2: Figure S8c), indicating that some RXLR effector genes in the TSGS isolates were repressed more heavily by sRNAs, which possibly contribute to less disease in TSGS. *Pi21422*, a

PexRD2 family member, accumulated more sRNAs in WNGZ than TSGS isolates (Fig. 4i). As a virulence factor, *Pi21422* interacts with the kinase domain of MAPKKKe to perturb plant defense signaling (King et al. 2014) and higher accumulation of sRNA in *Pi21422* may enhance the ability of the pathogen to evade host recognition, thereby reducing host defense in potatoes grown in WNGZ. Taken together, these results may help to explain the reduced severity of late blight in TSGS compared with WNGZ.

Promoters are known to activate gene transcription through the recognition by RNA polymerase. However, sRNAs can mimic the promoter and bind to the σ subunit of RNA polymerase, thereby altering the activity of RNA polymerase and affecting the transcription process (Caswell et al. 2014). In addition, sRNAs can also selectively interfere with gene promoter regions and accidentally activate gene transcription (Li et al. 2005), indicating that sRNAs can mediate gene silencing at the transcriptional level. We detected a large number of homologous sRNAs accumulating in the coding, upstream, and downstream of RXLR effector genes, even more sRNAs accumulation in promoter regions than that in the coding regions (Fig. 5a, b), and the homologous sRNA accumulation levels were also negatively correlated with the expression levels of RXLR effector genes, suggesting that significant sRNA enrichment is characteristic of RXLR effector genes in *P. infestans* and that epigenetics plays at least a similar role to genetics in regulating effector function.

The accumulation of homologous sRNAs within promoter regions of effector genes was regional specific. In total, 28 and 8 RXLR effector genes with significantly higher sRNAs accumulation were identified in TSGS and WNGZ isolates, respectively, and the expression of more RXLR effector genes may be inhibited in the TSGS isolates can partly explain their weaker virulence. Besides, ~50% of effector genes with different sRNA accumulation were consistently found in both gene bodies and regulatory regions (Additional file 2: Figure S8d). Taken these results together, we propose that sRNAs synthesis in the gene bodies and flanking regions of many effectors may be continuous and determined by a consistent epigenetic mechanism in the chromatin regions that regulate the transcription of the sRNA precursor.

Currently, 26 RXLR effector genes with virulence/avirulence have been reported. Among them, only the virulence factor *Pi21422* has been identified as a sRNA-associated effector gene. Regardless of whether it was in the gene region or in the promoter regulatory region, the homologous sRNA accumulation levels of these effector genes with known functions were consistently lower than those of sRNA-associated effector genes (Additional file 2: Figure S9). Taking the well-known *Avr3a* as an

example, its homologous sRNA accumulation level was significantly lower than the average accumulation levels of homologous sRNAs in both the sRNA-associated effector genes and entire effector genes (Additional file 2: Figure S9c, f). These results indicate that there may be some new effector genes in the tested isolates, and their differential expression is the cause of virulence variation of *P. infestans* isolates among regions. The finding of regional specific sRNA-associated effector genes provides both resource of discovering new effectors and clues for understanding the virulence variation, regional adaptation of *P. infestans*, as well as the effective utilization of resistant potato varieties.

Conclusions

We found spatial variations of RXLR effector genes at the genomic and transcriptional levels in *P. infestans* from TSGS and WNGZ even though extensive gene flow occurred between the two ecological regions, suggesting that local adaptation in *P. infestans* is associated with regional variations of RXLR effector genes. However, the underlying functional mechanisms of these eco-specific effector genes remain unknown but has important implications in understanding the adaptive landscape of pathogens such as *P. infestans* and for the selection and rational deployment of late blight resistance genes for sustainable disease management. This issue deserves further exploration.

Methods

Sampling and purification of *P. infestans* isolates

P. infestans isolates used in this study were collected from five sampling points in potato fields located at TSGS and WNGZ during the early stages of late blight onset according to the 'Zigzag' approach. The isolates were induced from infected potatoes with white mold on the back of leaves on potato tuber as described previously (Tian et al. 2016) and were grown on rye sucrose agar (RSA) medium plates at 16–18°C for 9–12 days. After 2–3 times of purification, the isolates were stored in liquid nitrogen until use.

Plant growth conditions and *P. infestans* infection assays

S. tuberosum plants were grown in a growth chamber at 23°C with a 16/8 h light/dark cycle. Potato leaves for seven-week-old potato were detached from the plants inoculated on the abaxial surfaces with a 16 µL droplet of spore suspension containing 800 zoospores. The inoculated leaves were incubated at 16–18°C for 3–6 days and lesion diameters were measured.

DNA extraction and SSR analysis

P. infestans isolates grown in RSA broth for 12–14 days at 16–18°C were harvested. Mycelia were quickly frozen with liquid nitrogen and stored at –80°C. DNA was extracted by *Phytophthora* DNA extraction solution (7 M Urea, 350 mM NaCl, 50 mM Tris-HCl, 4 mM EDTA-2Na, 1% Na-lauryl sarcosine, 1% Tris-Phenol), and the qualified DNA was stored at –20°C.

Five polymorphic SSR markers (SSR4, SSR6, SSR8, Pi4B, and Pi02; Lees et al. 2006; Li et al. 2012) were used to genotype the *P. infestans* isolates according to the protocol described previously (Kiiker et al. 2018). PCR products were separated by electrophoresis in polyacrylamide nondenaturing gel. After silver staining (1% AgNO₃), the gels were developed in 1.5% NaOH solution containing 0.1% formaldehyde until bands were clearly visible and repeatedly washed with distilled water and photographed. Band size was measured by DNA marker.

High-throughput sequencing

The library construction and sequencing of *P. infestans* genomic DNA were performed using the standard Illumina protocol by Biomarker Technologies (Beijing, CHN). Briefly, the qualified DNA samples were randomly broken into 350 bp fragments by Covaris, and TruSeq Library Construction Kit (Illumina, USA) was used to construct library. DNA fragments were sequenced on Illumina HiSeq 2500 platform.

Total RNA was extracted from the mycelia using TRIzol reagent according to the manufacturer's protocol (Invitrogen, USA). RNA-seq and sRNA-seq libraries were performed with PE150 on Illumina HiSeq Xten platform by Novogene (Beijing, CHN) with three biological replicates. RNA libraries and sRNA libraries were prepared using 1 µg of total RNA according to the protocols of RNA Library Prep Kit (New England Biolabs, USA) and Small RNA Library Prep Kit (Lexogen, Austria), respectively. For the construction of sRNA library, only 18–45 nt sRNAs were used for sequencing. The raw sequencing data was deposited in the Sequenced Read Archive (BioProject ID: PRJNA1059044).

Bioinformatic analysis

For whole genome resequencing data, quality control and filtering of raw data were performed using FastQC (v 0.11.6) and Trimmomatic-0.36 (-phred33 LEADING:3 TRAILING:3 SLIDINGWINDOW:4:15 MINLEN:36), respectively. The clean reads were mapped to the reference genome of *P. infestans* (T30-4; v 1.43) by BWA (v 0.7.15) with a seed length of 38 and a maximum of mismatches allowed of 1 (mem -t 4 -M -R). PCR duplications of each sample were removed from alignments using Picard (v 1.119). After indexing with Samtools (v 1.3.1), we

used the HaplotypeCaller tool from GATK (v 4.0) software to call variants and obtain gvcf files. The gvcf files from each sample were consolidated by the CombineGVCFs tool, ultimately resulting in a merged gvcf file. SNPs and InDels were extracted using the SelectVariants tool. Variant sites that represent the differences among the 19 strains were obtained by filtering out the SNPs/InDels that were consistent across all isolates based on the merged gvcf file. Picard (v 1.119), Samtools (v 1.3.1), and GATK (v 4.0) were used for PCR deduplication and SNP/InDel indexing and analysis, respectively. The upstream 1 kb sequence of genes was obtained by TBtools and used as the promoter regulatory sequences of the genes. To predict novel RXLR effector genes, unmapped reads of each isolate were extracted from genome alignments in SAM format by Samtools (v 1.3.1) were assembled using Velvet (v 1.2.10) with a Kmer of 30 to obtain contigs (-cov_cutoff 30 -ins_length 300 -ins_length_sd 100 -min_contig_lgth 200), and were then mapped to the reference genome using NUCmer (v 3.23; -c 200 -g 200 -p). After filtering out the contigs that were equivalent to the reference genome, the remaining contigs were retained for the search of open reading frames through an online website <http://emboss.bioinformatics.nl/cgi-bin/emboss/getorf>. Signal peptides and transmembrane domain of the candidate effectors were predicted using SignalP 4.1 (<https://services.healthtech.dtu.dk/services/SignalP-4.1/>) and TMHMM 2.0 (<https://services.healthtech.dtu.dk/services/TMHMM-2.0>), respectively. The detailed protocol for effector searching was as described by Cooke et al. (2012).

For RNA-seq data, raw sequencing reads were available through FastQC (v 0.11.6) and Trimmomatic-0.36. After removing adaptors and low-quality reads, the clean data were mapped to the reference genome of *P. infestans* using Hisat2 (v 2–2.0.3; -min-intronlen 20 -max-intronlen 3000). Gene expression was calculated using StringTie (v 1.3.3b; -e -B) and the expression level of genes was normalized by FPKM.

Cutadapt (v 2.9) was used to remove adapters from raw data and filter sRNAs with a length distribution between 18 and 45 nt (-m 18 -M 45). After trimming adaptors, the clean data were exactly mapped to *P. infestans* reference genome using Bowtie (v 1.1.2). No mismatch was allowed and all alignments for each read were reported (-f -v 0 -a -S). The sRNAs derived from ribosomal DNA (rDNA), mitochondrial DNA (mtDNA), and transfer RNA (tRNA) were identified and filtered out by Bowtie (v 1.1.2), allowing for a mismatch (-f -v 1 -a). The retained sRNAs were used for further analyses. Based on the alignment result and the genome annotation information, the sRNA

sequences with start positions falling within the gene region of candidate effectors, and their number was counted and normalized with RPKM (Jia et al. 2017).

Transient agroinfiltration assays

The selected *P. infestans* RXLR effector genes were amplified by primers (Additional file 1: Table S5) linked to the homology arms of the *EcoRI* and *XbaI* restriction sites and then ligated into the pART27-NGFP vector using homologous recombination. For ligation, *Agrobacterium tumefaciens* strain AGL1 containing plasmid constructs was grown for 24 h in LB medium at 28°C. The *A. tumefaciens* cells were collected by centrifugation and resuspended in infiltration buffer (10 mM MES, 10 mM MgCl₂, 0.2 mM acetosyringone, pH=5.6). After adjusting the *A. tumefaciens* suspensions (OD₆₀₀=0.3), Agro-infiltration assays were performed on leaves of 6 to 8-week-old *N. benthamiana* plants. After 24 h, leaves were detached and 800 zoospores (16 µL) of *P. infestans* were inoculated at the infiltration sites (Tian et al. 2016). Symptom development was monitored visually from 2 to 8 days after infiltration.

Quantitative RT-PCR analysis

Complementary DNA was synthesized using PrimeScript RT reagent Kit with gDNA Eraser (TaKaRa) according to the manufacturer's instructions. RT-qPCRs were performed with FastStart Universal SYBR Green Master (Roche). The *P. infestans* gene *PiU1BC* (*Pi08327*) was used as the reference gene. Gene expression relative to the reference gene was quantified using the 2^{-ΔΔCt} method. All specific primers used for RT-qPCR were listed in Additional file 1: Table S5.

Abbreviations

Co-IP	Co-immunoprecipitation
dpi	Days post infection
FPKM	Fragments per kilobase million
GSR	Gene sparse regions
Gt	Genotype
mtDNA	Mitochondrial DNA
PAV	Present or absent variations
PCA	Principal component analysis
rDNA	Ribosomal DNA
RPKM	Reads per kilobase per million mapped reads
RSA	Rye sucrose agar
RT-qPCR	Quantitative real-time polymerase chain reaction
RXLR	Arg-any amino acid-Leu-Arg
sRNA	Small RNA
SSR	Simple sequence repeat
tRNA	Transfer RNA
TSGS	Tianshui, Gansu
WNGZ	Weining, Guizhou

Supplementary Information

The online version contains supplementary material available at <https://doi.org/10.1186/s42483-024-00278-1>.

Additional file 1: Table S1. Origin and number of *P. infestans* isolates.

Table S2. *P. infestans* isolates used for high-throughput sequencing.

Table S3. *P. infestans* isolates successfully infected potato leaves. **Table S4.**

P. infestans genome re-sequencing data. **Table S5.** Primers used in this study. **Table S6.** Number of regional specific variations and RXLR effector genes under different criteria. **Table S7.** *P. infestans* sRNA-seq data.

Table S8. *P. infestans* RNA-seq data.

Additional file 2: Figure S1. Genotyping of *P. infestans* by five (SSR4, SSR6, SSR8, Pi4B, and Pi02) SSR markers. **a** Cluster graph based on *P. infestans* genotype. **b** Proportion of each *P. infestans* genotype in TSGS and WNGZ populations. Different colors represent different genotypes, and the dominant genotypes are marked with blue and red. **Figure S2.** Genetic structure and diversification of *P. infestans* populations in TSGS and WNGZ. **a** Phylogenetic tree of 19 isolates based on population SNPs. Blue and red represent the isolates from TSGS and WNGZ, respectively. **b** PCA analysis of two populations. **c** Distribution of *Fst* along the supercontigs of the genome. The value of *Fst* ranged from 0–1. 0 indicates a completely consistent genetic locus, and 1 indicates that alleles are fixed in different populations. **d** Comparison of pair-wise SNP abundance among isolates with different classification groups. Statistical significance was assessed by Student's *t*-test. ns, not significant. *** $P < 0.001$. **e** Phylogenetic tree of isolates based on haplotypes at RXLR effector genes. **Figure S3.** Sequence variation features of RXLR effector genes. **a, b** Number of SNPs (left) and InDels (right) in coding regions and promoter regions of effector genes in each isolate. The number above the black line represents the union of SNPs and InDels of all isolates from the same region. **c, d** Number and distribution of regional specific InDels in the coding regions and promoter regions. The histogram shows the number of InDels, and the colored grids represent the existence of InDels in the corresponding isolates. **e, f** Sequence alignment of known effector genes *Avr-Smira2*, *Avr-Smira1*, *Avr-amr1*, and *Pi22798* in TSGS and WNGZ isolates. **Figure S4.** Verification of RXLR effector gene expression pattern by RT-qPCR. **Figure S5.** Frequency of InDels in the promoter regions of *P. infestans* genes. The variants were called from the re-sequenced genomes of 19 isolates, and the 1 kp upstream sequence was regarded as the promoter region for each gene. **a** Frequency of InDels in the promoter regions of RXLR effector genes. **b** Frequency of InDels in the promoter regions of all genes. **Figure S6.** Expression and accumulation of sRNAs homologous to RXLR effector genes. **a, b** Ratio of effector gene with different expression levels and sRNA accumulation levels. **c** Number of common and regional specific RXLR effector genes between two regions. **Figure S7.** Verification of RXLR effector gene expression pattern by RT-qPCR. The histogram on the left shows the accumulation levels of sRNA homologous to effector genes, and the histogram on the right shows the expression levels of effector gene during infection. **Figure S8.** Total expression level and homologous sRNA accumulation level of RXLR effector genes. **a** Total abundance of homologous sRNAs in the upstream, downstream, and gene regions. **b** Total accumulation level of RXLR-derived sRNAs. **c** Total expression level of RXLR effector genes. **d** Proportion of effector genes that simultaneously accumulate homologous sRNAs in the coding regions and regulatory regions. **Figure S9.** Characteristics of homologous sRNAs accumulation of RXLR effector genes. **a, d** Accumulation level of sRNA homologous to sRNA-associated effectors in gene regions and promoter regions. **b, e** Accumulation level of sRNA homologous to reported effector genes in gene regions and promoter regions. **c, f** Accumulation level of sRNA homologous to *Avr3a* in gene region and promoter region. Statistical significance was assessed by Student's *t*-test. ns, not significant. *** $P < 0.001$.

Acknowledgements

We thank Lina Yang (Minjiang University, China) and Jinbu Jia (South China Agricultural University, China) for their insightful suggestions.

Author contributions

Conceptualization, WS, JZ, and JZ2; methodology, WS, JZ, and PT; validation, JZ and WL; investigation, JZ and YC; data curation, JZ and PT; writing original draft preparation, JZ; writing review and editing, WS, JZ, YM, and JZ2. All authors have read and agreed to the published version of the manuscript.

Funding

This work was supported by China Agriculture Research System (CARS-09), National Natural Science Foundation of China (31561143007), and the State Administration for Foreign Experts Affairs, PR China (B18042).

Availability of data and materials

Raw sequencing data is accessible under BioProject ID: PRJNA1059044.

Declarations

Ethical approval and consent to participate

Not applicable.

Consent for publication

Not applicable.

Competing interests

The authors declare that they have no competing interests.

Received: 28 May 2024 Accepted: 22 August 2024

Published online: 12 November 2024

References

- Åsman AK, Fogelqvist J, Vetukuri RR, Dixelius C. *Phytophthora infestans* Argonaute 1 binds microRNA and small RNAs from effector genes and transposable elements. *New Phytol.* 2016;211:993–1007. <https://doi.org/10.1111/nph.13946>.
- Bever JD, Platt TG, Morton ER. Microbial population and community dynamics on plant roots and their feedbacks on plant communities. *Annu Rev Microbiol.* 2012;66:265–83. <https://doi.org/10.1146/annurev-micro-092611-150107>.
- Cai J, Jiang Y, Ritchie ES, Macho AP, Yu F, Wu D. Manipulation of plant metabolism by pathogen effectors: more than just food. *FEMS Microbiol Rev.* 2023;47:faud007. <https://doi.org/10.1093/femsre/fuad007>.
- Castel SE, Martienssen RA. RNA interference in the nucleus: roles for small RNAs in transcription, epigenetics and beyond. *Nat Rev Genet.* 2013;14:100–12. <https://doi.org/10.1038/nrg3355>.
- Caswell CC, Oglesby-Sherrouse AG, Murphy ER. Sibling rivalry: related bacterial small RNAs and their redundant and non-redundant roles. *Front Cell Infect Microbiol.* 2014;4:151. <https://doi.org/10.3389/fcimb.2014.00151>.
- Chen XR, Zhang Y, Li HY, Zhang ZH, Sheng GL, Li YP, et al. The RXLR effector PcAvh1 is required for full virulence of *Phytophthora capsici*. *Mol Plant-Microbe Interact.* 2019;32:986–1000. <https://doi.org/10.1094/MPMI-09-18-0251-R>.
- Cheng YT, Zhang L, He SY. Plant-microbe interactions facing environmental challenge. *Cell Host Microbe.* 2019;26:183–92. <https://doi.org/10.1016/j.chom.2019.07.009>.
- Cooke DE, Cano LM, Raffaele S, Bain RA, Cooke LR, Etherington GJ, et al. Genome analyses of an aggressive and invasive lineage of the Irish potato famine pathogen. *PLoS Pathog.* 2012;8:e1002940. <https://doi.org/10.1371/journal.ppat.1002940>.
- Du Y, Weide R, Zhao Z, Msimuko P, Govers F, Bouwmeester K. RXLR effector diversity in *Phytophthora infestans* isolates determines recognition by potato resistance proteins; the case study AVR1 and R1. *Stud Mycol.* 2018;89:85–93. <https://doi.org/10.1016/j.simyco.2018.01.003>.
- Du Y, Chen X, Guo Y, Zhang X, Zhang H, Li F, et al. *Phytophthora infestans* RXLR effector PITG20303 targets a potato MKK1 protein to suppress plant immunity. *New Phytol.* 2021;229:501–15. <https://doi.org/10.1111/nph.16861>.

- El Kasmi F, Horvath D, Lahaye T. Microbial effectors and the role of water and sugar in the infection battle ground. *Curr Opin Plant Biol.* 2018;44:98–107. <https://doi.org/10.1016/j.pbi.2018.02.011>.
- Fischhoff IR, Huang T, Hamilton SK, Han BA, LaDeau SL, Ostfeld RS, et al. Parasite and pathogen effects on ecosystem processes: a quantitative review. *Ecosphere.* 2020. <https://doi.org/10.1002/ecs2.3057>.
- Gao F, Chen C, Li B, Weng Q, Chen Q. The gene flow direction of geographically distinct *Phytophthora infestans* populations in China corresponds with the route of seed potato exchange. *Front Microbiol.* 2020;11:1007. <https://doi.org/10.3389/fmicb.2020.01077>.
- Gilroy EM, Breen S, Whisson SC, Squires J, Hein I, Kaczmarek M, et al. Presence/absence, differential expression and sequence polymorphisms between PiAVR2 and PiAVR2-like in *Phytophthora infestans* determine virulence on R2 plants. *New Phytol.* 2011;191:763–76. <https://doi.org/10.1111/j.1469-8137.2011.03736.x>.
- Goel AK, Lundberg D, Torres MA, Matthews R, Akimoto-Tomiya C, Farmer L, et al. The *Pseudomonas syringae* type III effector HopAM1 enhances virulence on water-stressed plants. *Mol Plant-Microbe Interact.* 2008;21:361–70. <https://doi.org/10.1094/mpmi-21-3-0361>.
- Guo H, Zhou M, Zhang G, He L, Yan C, Wan M, et al. Development of homozygous tetraploid potato and whole genome doubling-induced the enrichment of H3K27ac and potentially enhanced resistance to cold-induced sweetening in tubers. *Hortic Res.* 2023;10:271–83. <https://doi.org/10.1093/hr/uhad017>.
- Haas BJ, Kamoun S, Zody MC, Jiang RH, Handsaker RE, Cano LM, et al. Genome sequence and analysis of the Irish potato famine pathogen *Phytophthora infestans*. *Nature.* 2009;461:393–8. <https://doi.org/10.1038/nature08358>.
- Huang L, Mei X, Li X, Li X, Zu Y, He Y, et al. Effects of UV-B radiation on the expression of four pathogenic genes in the infection stage of *Magnaporthe grisea*. *J Agro-Environ Sci.* 2019;38:494–501. <https://doi.org/10.11654/jaes.2018-0625>.
- Huot B, Castroverde CD, Velásquez AC, Hubbard E, Pulman JA, Yao J, et al. Dual impact of elevated temperature on plant defence and bacterial virulence in Arabidopsis. *Nat Commun.* 2017;8:1808. <https://doi.org/10.1038/s41467-017-01674-2>.
- Jia J, Lu W, Zhong C, Zhou R, Xu J, Liu W, et al. The 25–26 nt small RNAs in *Phytophthora parasitica* are associated with efficient silencing of homologous endogenous genes. *Front Microbiol.* 2017;8:773. <https://doi.org/10.3389/fmicb.2017.00773>.
- Khavkin EE. Plant-pathogen molecular dialogue: evolution, mechanisms and agricultural implementation. *Russ J Plant Physiol.* 2021;68:197–211. <https://doi.org/10.1134/s1021443721020072>.
- Kiiker R, Hansen M, Williams IH, Cooke DE, Runno-Paurson E. Outcome of sexual reproduction in the *Phytophthora infestans* population in Estonian potato fields. *Eur J Plant Pathol.* 2018;152:395–407. <https://doi.org/10.1007/s10658-018-1483-y>.
- King SR, McLellan H, Boevink PC, Armstrong MR, Bukharova T, Sukarta O, et al. *Phytophthora infestans* RXLR effector PexRD2 interacts with host MAPKKK epsilon to suppress plant immune signaling. *Plant Cell.* 2014;26:1345–59. <https://doi.org/10.1105/tpc.113.120055>.
- Lal M, Chaudhary S, Yadav S, Sharma S, Charabarti SK, Kumar M. Development of spray schedules for management of late blight of potato using new chemicals. *J Mycol Plant Pathol.* 2019;49:405–12.
- Lees AK, Wattier R, Shaw DS, Sullivan L, Williams NA, Cooke DE. Novel microsatellite markers for the analysis of *Phytophthora infestans* populations. *Plant Pathol.* 2006;55:311–9. <https://doi.org/10.1111/j.1365-3059.2006.01359.x>.
- Li L, Okino ST, Zhao H, Pookot D, Urakami S, Enokida H, et al. Small interfering RNA directed transcriptional activation in human cells. *Cancer Res.* 2005;65:1436.
- Li Y, van der Lee TA, Evenhuis A, van den Bosch GB, van Bekkum PJ, Förch MG, et al. Population dynamics of *Phytophthora infestans* in the Netherlands reveals expansion and spread of dominant clonal lineages and virulence in sexual offspring. *G3-Genes Genom Genet.* 2012;2:1529–40. <https://doi.org/10.1534/g3.112.004150>.
- MacDonald ZG, Dupuis JR, Davis CS, Acorn JH, Nielsen SE, Sperling FA. Gene flow and climate-associated genetic variation in a vagile habitat specialist. *Mol Ecol.* 2020;29:3889–906. <https://doi.org/10.1111/mec.15604>.
- Mainwaring JC, Vink J, Gerth M. Plant-pathogen management in a native forest ecosystem. *Curr Biol.* 2023;33:R500–5. <https://doi.org/10.1016/j.cub.2023.02.047>.
- Mandal K, Dutta S, Upadhyay A, Panda A, Tripathy S. Comparative genome analysis across 128 *Phytophthora* isolates reveal species-specific microsatellite distribution and localized evolution of compartmentalized genomes. *Front Microbiol.* 2022;13:806398. <https://doi.org/10.3389/fmicb.2022.806398>.
- Marguet E, Forterre P. DNA stability at temperatures typical for hyperthermophiles. *Nucleic Acids Res.* 1994;22:1681–6. <https://doi.org/10.1093/nar/22.9.1681>.
- Matsuba C, Ostrow DG, Salomon MP, Tolani A, Baer CF. Temperature, stress and spontaneous mutation in *Caenorhabditis briggsae* and *Caenorhabditis elegans*. *Biol Lett.* 2013;9:20120334. <https://doi.org/10.1098/rsbl.2012.0334>.
- Ngou BP, Ding P, Jones JD. Thirty years of resistance: zig-zag through the plant immune system. *Plant Cell.* 2022;34:1447–78. <https://doi.org/10.1093/plcell/koac041>.
- Phan HT, Rybak K, Furuki E, Breen S, Solomon PS, Oliver RP, et al. Differential effector gene expression underpins epistasis in a plant fungal disease. *Plant J.* 2016;87:343–54. <https://doi.org/10.1111/tpj.13203>.
- Qutob D, Chapman BP, Gijzen M. Transgenerational gene silencing causes gain of virulence in a plant pathogen. *Nat Commun.* 2013;4:1349. <https://doi.org/10.1038/ncomms2354>.
- Rastogi RP, Richa, Kumar A, Tyagi MB, Sinha RP. Molecular mechanisms of ultraviolet radiation-induced DNA damage and repair. *J Nucleic Acids.* 2010;2010:592980. <https://doi.org/10.4061/2010/592980>.
- Rehmany AP, Gordon A, Rose LE, Allen RL, Armstrong MR, Whisson SC, et al. Differential recognition of highly divergent downy mildew avirulence gene alleles by RPP1 resistance genes from two Arabidopsis lines. *Plant Cell.* 2005;17:1839–50. <https://doi.org/10.1105/tpc.105.031807>.
- Rietman H, Bijsterbosch G, Cano LM, Lee HR, Vossen JH, Jacobsen E, et al. Qualitative and quantitative late blight resistance in the potato cultivar *Sarpo Mira* is determined by the perception of five distinct RXLR effectors. *Mol Plant-Microbe Interact.* 2012;25:910. <https://doi.org/10.1094/mpmi-01-12-0010-r>.
- Shen L, Waheed A, Wang Y, Nkurikiyimfura O, Wang Z, Yang L, et al. Multiple mechanisms drive the evolutionary adaptation of *Phytophthora infestans* effector Avr1 to host resistance. *J Fungi.* 2021;7:789. <https://doi.org/10.1016/j.sjmyco.2018.01.003>.
- Shibai A, Takahashi Y, Ishizawa Y, Motooka D, Nakamura S, Ying BW, et al. Mutation accumulation under UV radiation in *Escherichia coli*. *Sci Rep-UK.* 2017;7:14531. <https://doi.org/10.1038/s41598-017-15008-1>.
- Singh AK, Sad K, Singh SK, Shivaji S. Regulation of gene expression at low temperature: role of cold-inducible promoters. *Microbiology.* 2014;160:1291–7. <https://doi.org/10.1099/mic.0.077594-0>.
- Snelders NC, Rovenich H, Petti GC, Rocafort M, van den Berg GC, Vorholt JA, et al. Microbiome manipulation by a soil-borne fungal plant pathogen using effector proteins. *Nat Plants.* 2020;6:1365–74. <https://doi.org/10.1038/s41477-020-00799-5>.
- Tian Y, Yin J, Sun J, Ma Y, Wang Q, Quan J, et al. Population genetic analysis of *Phytophthora infestans* in northwestern China. *Plant Pathol.* 2016;65:17–25. <https://doi.org/10.1111/ppa.12392>.
- Todd JN, Carreón-Anguiano KG, Islas-Flores I, Canto-Canché B. Microbial effectors: key determinants in plant health and disease. *Microorganisms.* 2022;10:1980. <https://doi.org/10.3390/microorganisms10101980>.
- Ulse S, Djamei A. Effectors of plant-colonizing fungi and beyond. *PLoS Pathog.* 2018;14:e1006992. <https://doi.org/10.1371/journal.ppat.1006992>.
- Velásquez AC, Castroverde CD, He SY. Plant-pathogen warfare under changing climate conditions. *Curr Biol.* 2018;28:R619–34. <https://doi.org/10.1016/j.cub.2018.03.054>.
- Vetukuri RR, Avrova AO, Grenville-Briggs LJ, West PV, Söderbom F, Savenkov EI, et al. Evidence for involvement of Dicer-like, Argonaute and histone deacetylase proteins in gene silencing in *Phytophthora infestans*. *Mol Plant Pathol.* 2011;12:772–85. <https://doi.org/10.1111/j.1364-3703.2011.00710.x>.
- Vetukuri RR, Åsman AK, Tellgren-Roth C, Jahan SN, Reimegård J, Fogelqvist J, et al. Evidence for small RNAs homologous to effector-encoding genes and transposable elements in the oomycete *Phytophthora infestans*. *PLoS ONE.* 2012;7:e51399. <https://doi.org/10.1371/journal.pone.0051399>.
- Vleeshouwers VG, Oliver RP. Effectors as tools in disease resistance breeding against biotrophic, hemibiotrophic, and necrotrophic plant pathogens. *Mol Plant-Microbe Interact.* 2014;27:196–206. <https://doi.org/10.1094/MPMI-10-13-0313-IA>.
- Waheed A, Wang Y, Nkurikiyimfura O, Li W, Liu S, Lurwanu Y, et al. Effector Avr4 in *Phytophthora infestans* escapes host immunity mainly through early termination. *Front Microbiol.* 2021;12:646062. <https://doi.org/10.3389/fmicb.2021.646062>.
- Wang Q, Li T, Zhong C, Luo S, Xu K, Gu B, et al. Small RNAs generated by bidirectional transcription mediate silencing of RXLR effector genes in the

- oomycete *Phytophthora sojae*. *Phytopathology Res.* 2019;1:1–11. <https://doi.org/10.1186/s42483-019-0026-6>.
- Wang L, Chen H, Li J, Shu H, Zhang X, Wang Y, et al. Effector gene silencing mediated by histone methylation underpins host adaptation in an oomycete plant pathogen. *Nucleic Acids Res.* 2020;48:1790–9. <https://doi.org/10.1093/nar/gkz1160>.
- Wang Z, Li T, Zhang X, Feng J, Liu Z, Shan W, et al. A *Phytophthora infestans* RXLR effector targets a potato ubiquitin-like domain-containing protein to inhibit the proteasome activity and hamper plant immunity. *New Phytol.* 2023;238:781–97. <https://doi.org/10.1111/nph.18749>.
- Xin X, Nomura K, Aung K, Velásquez AC, Yao J, Boutrot F, et al. Bacteria establish an aqueous living space in plants crucial for virulence. *Nature.* 2016;539:524–9. <https://doi.org/10.1038/nature20166>.
- Xu J, Li Y, Jia J, Xiong W, Zhong C, Huang G, et al. Mutations in PpAGO3 lead to enhanced virulence of *Phytophthora parasitica* by activation of 25–26 nt sRNA-associated effector genes. *Front Microbiol.* 2022;13:856106. <https://doi.org/10.3389/fmicb.2022.856106>.
- Yang L, Ouyang H, Fang Z, Zhu W, Wu E, Luo G, et al. Evidence for intragenic recombination and selective sweep in an effector gene of *Phytophthora infestans*. *Evol Appl.* 2018;11:1342–53. <https://doi.org/10.1111/eva.12629>.
- Yang L, Liu H, Duan G, Huang Y, Liu S, Fang Z, et al. The *Phytophthora infestans* AVR2 effector escapes R2 recognition through effector disordering. *Mol Plant-Microbe Interact.* 2020;33:921–31. <https://doi.org/10.1094/mpmi-07-19-0179-r>.
- Yang L, Ouyang H, Nkurikiyimfura O, Fang H, Waheed A, Li W, et al. Genetic variation along an altitudinal gradient in the *Phytophthora infestans* effector gene *Pi02860*. *Front Microbiol.* 2022;13:972928. <https://doi.org/10.3389/fmicb.2022.972928>.
- Zhang T, Zhao Y, Zhao J, Wang S, Jin Y, Chen Z, et al. Cotton plants export micro-RNAs to inhibit virulence gene expression in a fungal pathogen. *Nat Plants.* 2016;2:16153. <https://doi.org/10.1038/nplants.2016.153>.
- Zhang X, Liu B, Zou F, Shen D, Yin Z, Wang R, et al. Whole genome re-sequencing reveals natural variation and adaptive evolution of *Phytophthora sojae*. *Front Microbiol.* 2019;10:2792. <https://doi.org/10.3389/fmicb.2019.02792>.